PHYSICAL REVIEW B **78**, 012405 (2008)

Voltage-controlled surface magnetization of itinerant ferromagnet $Ni_{1-x}Cu_x$

Igor V. Ovchinnikov* and Kang L. Wang†
Department of Electrical Engineering, University of California at Los Angeles, Los Angeles, California, 90066, USA

(Received 21 June 2008; published 15 July 2008)

We argue that surface magnetization of a metallic ferromagnet can be turned on and off isothermally by an applied voltage. For this, the material's electron subsystem must be close enough to the boundary between paramagnetic and ferromagnetic regions on the electron density scale. For the 3*d* series, the boundary is between Ni and Cu, which makes their alloy a primary candidate. Using Ginzburg-Landau functional, which we build from $Ni_{1-x}Cu_x$ empirical properties, *ab-initio* parameters of Ni and Cu, and orbital-free LSDA, we show that the proposed effect is experimentally observable.

DOI: 10.1103/PhysRevB.78.012405 PACS number(s): 85.75.−d, 85.70.Ay

Further evolution of magnetoelectronics[1] depends highly on the availability of materials in which local magnetization can be turned on and off isothermally by an electric voltage. The hopes to achieve this are mainly laid on the dilute magnetic semiconductors (DMS),[2] in which the effect was recently demonstrated experimentally.[3] The voltage-controlled ferromagnetic ordering in DMS relies on the virtue of doped semiconductors to allow external variation of the free-carrier spatial density within the semiconductor depletion layer, typically measured in dozens of nanometers. The voltage variation of the high electron density in metals is possible only within the atomic size Thomas-Fermi (TF) surface layer. As a result, the voltage-controlled ferromagnetism in a metal has not been considered a possibility lately.

We argue that by capacitively charging a metallic ferromagnet, one can drive the surface electron subsystem in and out of its ferromagnetic state. At this, the electron system of the metal has to be paramagnetic at the device operation temperature (room temperature T_0), but close enough to the ferromagnetic state on the temperature and/or electron density scales. The proximity of the ferromagnetic transition will play a twofold role: (i) the capacitive change in the electron density is relatively small so that the transition has to be sufficiently close in order to reach the ferromagnetic region with reasonable voltages, and (ii) due to the critical collective spin correlations, the spin-correlation length grows infinitely as one approaches the transition point. Consequently, even though the injected carriers are spatially limited to the TF layer, the system must develop a much wider surface magnetization profile. In this paper we investigate the proposed possibility in $Ni_{1-x}Cu_x$.

The nature of ferromagnetism lies in the competition between the kinetic energy and the exchange interaction. The kinetic energy of the spatial quantization tends to equalize the numbers of spin up and down electrons by shifting the fermionic antisymmetry into the spin sector of the many-body wave function. In turn, the exchange interaction does the opposite, struggling to unbalance the up and down spins. For itinerant ferromagnets, the subclass of materials elemental ferromagnets belong to, the outcome of this competition can be predicted from the Stoner criterion.[4] According to the Stoner criterion, ferromagnets possess a high density of states (DOS) at the (paramagnetic) chemical potential. In the 3*d* series, the high DOS is provided by the 3*d* band on the background of the low and wide 4*s* and 4*p* bands [see Fig. 1(a)]. Thus, the elements with the chemical potential within the 3*d* band, Fe, Co, and Ni, are ferromagnetic, whereas the very next element, Cu, is not. Cu has an extra electron per atom beyond Ni so that on the electron density scale, the ferro-to-para boundary lies between Ni and Cu.

Despite their different magnetic properties, Ni and Cu are very similar from the band structure point of view. In a crystalline state both form the face-centered cubic lattice with almost the same lattice constant, *a* (6.69 vs 6.83 a.u.). In result, on alloying, Ni and Cu form substitutional solid solutions at all compositions. Consequently, $Ni_{1-x}Cu_x$ can be thought of as an all-the-same structure solid, with the equilibrium electron density varying linearly with x, $\rho_0 = \rho_{Ni} + x/a^3$. Within this picture, x and ρ_0 are interchangeable.

Other experimentally observed properties of the alloy[5] can be well approximated as [see Figs. 1(b)–1(d)] the linear dependence of the zero-temperature spin density $s_0(\rho_0, 0)$, the Curie temperature $T_C(\rho_0)$ on ρ_0, and the Landau depen-

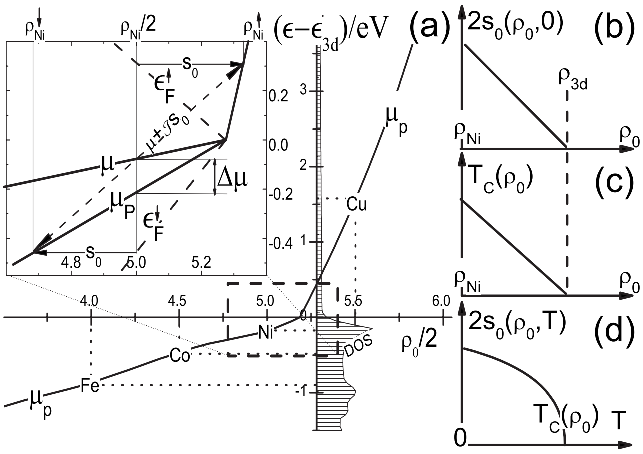

FIG. 1. (a) Schematics showing the paramagnetic chemical potentials of the elemental ferromagnets on the kinetic energy, ϵ, and the spatial electron density, ρ_0 (outer shell electrons per atom), scales. The inset is the magnified dashed area, which shows the graphic solution for Eq. (3) determining the spin density, s_0, the paramagnetic and ferromagnetic chemical potentials, μ_P and μ, and the spin up and down *kinetic* Fermi energies, $\epsilon_F^{\uparrow\downarrow}$, as functions of ρ_0 for pure Ni, $\rho_0 = \rho_{Ni}$. (b)–(d) The experimentally observed properties of $Ni_{1-x}Cu_x$: (b) zero-temperature magnetization vs ρ_0; (c) Curie temperature vs ρ_0; (d) the magnetization vs temperature, T.

dence of the spin density $s_0(\rho_0,T)$ on temperature T:

$$2s_0(\rho_0,0)/\gamma=(\rho_{3d}-\rho_0)\,\theta(\rho_{3d}-\rho_0), \tag{1a}$$

$$T_C(\rho_0)/\kappa=(\rho_{3d}-\rho_0)\,\theta(\rho_{3d}-\rho_0), \tag{1b}$$

$$s_0(\rho_0,T)/s_0(\rho_0,0)=(1-\tilde{T})^{1/2}\theta(\rho_{3d}-\rho_0), \tag{1c}$$

where $\tilde{T}=T/T_C(\rho_0)$, θ is the Heaviside step function, $\rho_{3d}=\rho_{\mathrm{Ni}}+0.53/a^3$ is the position of the $3d$ band edge on the density scale, and γ and κ are the slopes of the $2s_0(\rho_0,0)$ and $T_C(\rho_0)$ lines. For nickel $2s_0(\rho_{\mathrm{Ni}},0)=0.66/a^3$ and $T_C(\rho_{\mathrm{Ni}})=627$ K so that $\gamma\approx1.25$ and $\kappa\approx1.2\times10^2$ Ka^3.

A rather accurate quantitative look at the itinerant ferromagnetism can be taken via the Stoner approximation.[4] In a homogeneous system case, the zero-temperature energy per volume is the sum of the kinetic and exchange parts:

$$\mathcal{E}_{\mathcal{KX}}(\rho_0,s_0)=\sum\nolimits_{\uparrow\downarrow}\mathcal{K}(\rho_0^{\uparrow\downarrow})-\mathcal{J}s_0^2, \tag{2}$$

where $\rho_0^{\uparrow\downarrow}=\rho_0/2\pm s_0$ are the up and down spin densities, $\mathcal{J}$ is the Heisenberg exchange interaction constant,[6] and the kinetic energy is defined as $\mathcal{K}(\rho_0^{\uparrow\downarrow})=\int_{-\infty}^{\epsilon_F^{\uparrow\downarrow}}\epsilon'\nu(\epsilon')d\epsilon'$, with $\epsilon_F^{\uparrow\downarrow}\equiv\epsilon_F(\rho_0^{\uparrow\downarrow})$ being the *kinetic* spin up and down Fermi energies, and ν being the DOS (per spin).[7] The function ϵ_F defines the one-to-one correspondence between the (spin) density and the position of the Fermi energy on the kinetic energy scale. It can be defined via its inverse function as $\rho=\int_{-\infty}^{\epsilon_F}\nu(\epsilon')d\epsilon'$ so that $\partial\epsilon_F/\partial\rho=\nu(\epsilon_F)^{-1}$ and $\partial\mathcal{K}/\partial\rho=\epsilon_F$, i.e., ϵ_F and ρ are the Legandre conjugates with respect to $\mathcal{K}$.

For the ground state, vanishing variations of $\mathcal{E}_{\mathcal{KX}}$ in ρ_0 and s_0 yield the equations determining the ground state's spin density and the chemical potential as functions of ρ_0:

$$2s_0(\rho_0)\mathcal{J}=\epsilon_F^{\uparrow}-\epsilon_F^{\downarrow},\mu(\rho_0)=(\epsilon_F^{\uparrow}+\epsilon_F^{\downarrow})/2. \tag{3}$$

To get Eq. (1) from Eq. (3) [the graphic solution for pure Ni is given in the inset of Fig. 1(a)], the DOS has to be of the following simple form (ϵ_{3d} is the $3d$ band edge):

$$\nu(\epsilon)=\nu_{\mathrm{Ni}}\theta(\epsilon_{3d}-\epsilon)+\nu_{\mathrm{Cu}}\theta(\epsilon-\epsilon_{3d}).$$

Then,

$$\gamma=(\nu_{\mathrm{Cu}}^{-1}-\nu_{\mathrm{Ni}}^{-1})/(\nu_{\mathrm{Ni}}^{-1}+\nu_{\mathrm{Cu}}^{-1}-2\mathcal{J})$$

and

$$\mu(\rho_0)=\mu_P(\rho_0)-\Delta\mu(\rho_0), \tag{4}$$

where

$$\mu_P(\rho_0)=\epsilon_{3d}+\frac{1}{2}(\rho_0-\rho_{3d})\times\begin{cases}\nu_{\mathrm{Ni}}^{-1}, & \rho_0<\rho_{3d},\\ \nu_{\mathrm{Cu}}^{-1}, & \rho_0>\rho_{3d},\end{cases} \tag{5}$$

is the chemical potential corresponding to the paramagnetic solution [$s_0=0$, $\mu_{\mathrm{P}}=\mu=\epsilon_F^{\uparrow\downarrow}=\epsilon_F(\rho_0/2)$], and

$$\Delta\mu(\rho_0)=(2\Delta\nu)^{-1}(\rho_0-\rho_{3d})\,\theta(\rho_{3d}-\rho_0), \tag{6}$$

is the chemical potential shift due to the switching from the paramagnetic to the ferromagnetic state, with $\Delta\nu^{-1}=\gamma(\mathcal{J}-\nu_{\mathrm{Ni}}^{-1})$.[8] Numerical estimates for the parameters of the model can be obtained by fitting $\mu_P(\rho_{\mathrm{Ni,Cu}})-\epsilon_{3d}$ from Eq. (5) and the exchange spitting in Ni, $2s_0(\rho_{\mathrm{Ni}})\mathcal{J}$, with their *ab-initio* values:[9] $\nu_{\mathrm{Cu,Ni}}^{-1}=6.7$, 0.79 eV$a^3$, $\mathcal{J}=1.3$ eVa^3, and $\Delta\nu^{-1}=0.61$ eVa^3.

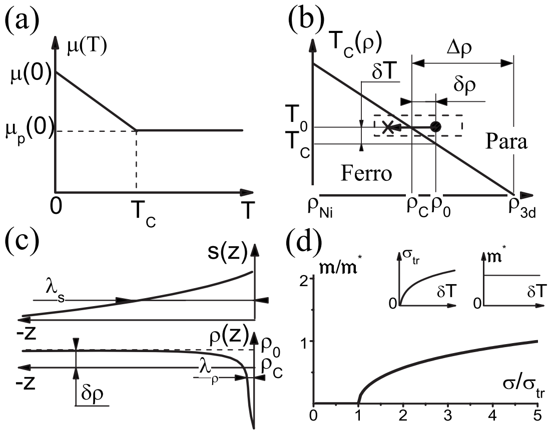

FIG. 2. (a) The chemical potential provided by the proposed model vs temperature. (b) The area on the (T,ρ) plane under consideration (dashed rectangle). The parameters $\Delta\rho$, ρ_C,$\delta\rho$, and δT are introduced in the text. The arrow symbolizes the effect of the (positive) bias on the surface electron subsystem. (c) The widths of the spatial profiles of the magnetization and the density are determined by the spin and density correlation lengths [Eq. (9)], and $\lambda_s\gg\lambda_\rho$. (d) The surface magnetization, $\mathfrak{M}$, vs surface charge, σ. (Insets) The threshold charging, σ_{tr}, and the characteristic magnetization, $\mathfrak{M}^*$, vs the alloy's detuning from the transition, δT.

For nonzero temperatures, the free energy of a homogeneous system can be assumed a function of ρ_0, s_0, and T. Its spatial density can be given as the sum of the paramagnetic and ferromagnetic (Landau) parts

$$\mathcal{F}_{\mathcal{KX}}(\rho_0,s_0,T)=\mathcal{F}_P(\rho_0,T)+\Delta\mathcal{F}(\rho_0,s_0,T). \tag{7a}$$

$\mathcal{F}_P$ is determined mostly by the crystal structure. For not very high temperatures, such that all the structural phase transitions are far on the (T,ρ) plane, $\mathcal{F}_p$ can be assumed temperature independent and consequently equal to the paramagnetic part of the zero-temperature energy so that $\partial_{\rho_0}\mathcal{F}_P=\mu_P(\rho_0)$.

The ferromagnetic properties of the alloy [Eqs. (1a)–(1c)] determine the Landau part of the free energy up to an unknown factor f:

$$\Delta\mathcal{F}=f[2(\rho_0-\rho_{3d})^2(\tilde{T}-1)(2s_0/\gamma)^2+(2s_0/\gamma)^4]. \tag{7b}$$

The para-to-ferro shift of the chemical potential provided by ΔF is

$$\Delta\mu(\rho_0,T)=-\partial_{\rho_0}[f(\rho_0-\rho_{3d})^4(\tilde{T}-1)^2]\theta(1-\tilde{T}).$$

The comparison of the previous equation at $T=0$ with Eq. (6), together with the assumption that f is also temperature independent, uniquely defines the function f

$$f(\rho_0)=(\rho_0-\rho_{3d})^{-2}/(4\Delta\nu). \tag{7c}$$

Accordingly, $\Delta\mu(\rho_0,T)=\Delta\mu(\rho_0)(1-\tilde{T})\theta(1-\tilde{T})$, with $\Delta\mu(\rho_0)$ from Eq. (6) [see Fig. 2(a)].

Now, in the spirit of the orbital-free local spin density approximation (LSDA), we turn to an inhomogeneous case by letting the electron and the spin densities spatially vary: $\rho_0 \to \rho(\boldsymbol{x})$, $s_0 \to s(\boldsymbol{x})$. Capacitively charging the conductor we make it an open system, which is governed by the Ω functional

$$\Omega = \int d^3\boldsymbol{x}(\mathcal{W} + \mathcal{F}_{\mathcal{K}\mathcal{X}} - \mu_0\rho + e\varphi(\rho - \rho_0)/2). \tag{8a}$$

Here $\mathcal{F}_{\mathcal{K}\mathcal{X}}$ is defined by Eqs. (7a) and (7c), $\mu_0 \equiv \mu(\rho_0, T_0)$, $\varphi = e\int d^3\boldsymbol{x}'(\rho(\boldsymbol{x}') - \rho_0)/|\boldsymbol{x} - \boldsymbol{x}'|$ is the direct interaction potential with e being the electron charge, and the nonlocality of the kinetic energy functional is accounted for by the α von Weiszacker term,[10] $\mathcal{W} = \alpha\hbar^2/(8m^*)\Sigma_{\uparrow\downarrow}(\boldsymbol{\nabla}\rho^{\uparrow\downarrow})^2/\rho_h^{\uparrow\downarrow}$, with m^* being the effective mass of the $3d$ holes and with $\rho_h^{\uparrow\downarrow} \equiv \rho_{3d}/2 - \rho^{\uparrow\downarrow}$ being the spin up and down hole densities. We adopt $\alpha = 1/9$, the case when the α von Weiszacker approximation is asymptotically correct for long wavelengths,[11] i.e., the domain of the applicability of the Ginzburg-Landau (GL) theory below.

As we already mentioned, the TF layer's spatial electron density variation, due to the injection of the carriers, is relatively small. Therefore, to be able to reach the ferromagnetic region from an initially paramagnetic state, we need an alloy which is close to its transition at T_0—$T_C \equiv T_C(\rho_0) < T_0$, $\delta T = T_0 - T_C \ll T_0$ [see Fig. 2(b)]—so that $\delta\rho = \rho_0 - \rho_C = \delta T/\kappa \ll \Delta\rho$, where $\rho_C = \rho_{3d} - \Delta\rho$ and $\Delta\rho = T_0/\kappa \approx 0.25/a^3$. Having chosen the composition, we can focus on a small area on (ρ, T) plane, such that $|\rho - \rho_C| \ll \Delta\rho$. Within the area, $\rho_h^{\uparrow\downarrow} \approx \Delta\rho/2$, and the von Weiszacker term simplifies as

$$\mathcal{W} \approx \alpha\hbar^2[(\boldsymbol{\nabla}\rho)^2 + 4(\boldsymbol{\nabla}s)^2]/(8m^*\Delta\rho). \tag{8b}$$

In the Thomas-Fermi picture of a Fermi liquid, which the von Weiszacker correction relies on, the DOS at the chemical potential is given as $\nu_{\mathrm{TF}} = k_F m^*/(2\pi^2\hbar^2)$, where $k_F = (3\pi^2\Delta\rho)^{1/3}$ is the Fermi wave vector. To make the von Weiszacker term energywise consistent with the rest of the Ω potential obtained by the physical arguments different from the orbital-free LSDA, we can require that $\nu_{\mathrm{TF}} = \nu_{\mathrm{Ni}}$, or $m^* \approx 8.2m_0$. This value of the effective mass lies well within the wide range of the $3d$ sub-bands' effective masses, which vary from several m_0 to almost $30m_0$ (see, e.g., Ref. 12).

Even though the orbital-free LSDA has proven successful in some atomic-scale nonhomogeneous problems, in our case any atomic-scale results obtained from Eqs. (8) would have a rather qualitative character. Indeed, the very notion of the composition of a solid solution is well defined only on scales larger than the lattice constant. Furthermore, the microscopic properties of the electron subsystem of the TF layer differ from those of the bulk and are interface-material dependent. The Ω potential [Eq. (8)], however, can be used to find the characteristic distances of the spatial variations of ρ and s, which are given by the density and the spin correlation lengths, λ_ρ and λ_s. Omitting intermediate derivations, the correlation lengths obtained from Eq. (8) in a linear response manner are

$$\lambda_\rho = 2^{-1/2}\lambda_{\mathrm{TF}}\,\mathrm{Re}\sqrt{1 + \sqrt{1 - k_F/(\pi^2\Delta\rho\lambda_{\mathrm{TF}}^2)}}, \tag{9a}$$

$$\lambda_s = \lambda_\rho(\Lambda/\delta T)^{1/2}. \tag{9b}$$

Here the Thomas-Fermi radius $\lambda_{\mathrm{TF}} = [4\pi e^2(2\nu_{\mathrm{Ni}})]^{-1/2}$ and $\Lambda = \alpha\kappa\gamma^2\Delta\nu/(4m^*\lambda_\rho^2)$.

The numerical estimations lead to $\Lambda \approx 7 \times 10^2$ K. In the vicinity of the transition, the inequality $\delta T \ll \Lambda$ is well satisfied so that the spin and the density scale separate, $\lambda_s \gg \lambda_\rho$ [see Eq. (9b)]. Thus, we arrived at a typical picture of the critical phenomena theory. The spin density is a "ready-to-condense" *soft* variable, behavior of which is governed by the large-scale low-energy GL functional [the s-dependent part of Eq. (8)], which in the (T, ρ), the area under consideration, has the following form:

$$\mathcal{F}_{\mathrm{GL}} = \int d^3\boldsymbol{x}[A(\boldsymbol{\nabla}s)^2 + b(\rho - \rho_C)s^2 + Cs^4/2], \tag{10}$$

with $b = 2/(\gamma^4\Delta\rho\Delta\nu)$, $A = k_s b$, $C = 4b/(\gamma^2\Delta\rho)$. The high-energy *stiff* variable, ρ, plays a guiding role via the ρ dependence of the effective chemical potential for the magnetization [the overall coefficient in s^2 term of Eq. (10), $B = b(\rho - \rho_C)$]. The feedback action of the soft variable, s, on the stiff variable, ρ, is weak and/or unimportant.

The proposed form of the near-critical s-ρ coupling can be obtained on a more general footing. Indeed, Taylor expanding B around the transition point at which $B(T_0, \rho_0) = 0$, and noticing that in itinerant ferromagnets the s-ρ coupling can only be local (especially on the λ_s scale), we arrive at $B \approx b(\rho - \rho_0) + b'(T_0 - T_C) \equiv b(\rho - \rho_C)$, with $\rho_C = \rho_0 - \delta\rho$, $\delta\rho = (T_0 - T_C)/\kappa$, $\kappa \equiv b/b'$. For quantitative studies, however, it is crucial to possess reliable values of the three material-specific parameters for Eq. (10). The way the parameters for $\mathrm{Ni}_{1-x}\mathrm{Cu}_x$ are derived in this Brief Report can now be summarized as follows: A is obtained from the orbital-free LSDA considerations [Eq. (8b)]; the mutual relation between b and C from the empirical properties of the alloy and from the Landau theory for the II-order phase transitions [Eq. (7b)]; the overall energy factor for b and C from previous *ab-initio* parameters of Ni and Cu and from the Stoner theory of itinerant ferromagnetism [Eqs. (6) and (7c)].

On the λ_s scale, the microscopic effects are scaled out. The magnetization is ignorant to the microscopic details of the electron density profile, e.g., the Friedel oscillations. The injected carriers' spatial density in the TF layer, with a width of the order of λ_ρ, can be assumed infinitely narrow. Therefore, a positively-biased surface can be represented as a one-dimensional (1D) semi-infinite solution [$z < 0$, see Fig. 2(c)] of the GL Euler equation with $\rho(\boldsymbol{x}) \to \rho_0$ and with the following boundary condition imposed by the form of the s-ρ coupling: $\lambda_s\,\partial_z \ln s|_{z=0} = \sigma/\sigma_{\mathrm{tr}}$, where $\sigma = -\int_{-\infty}^{0}(\rho(z) - \rho_0)dz$ is the surface density of the excess holes and $\sigma_{\mathrm{tr}} = \lambda_s\delta\rho$ is the threshold charging. The solution is $s = s^*\{\sinh[\coth^{-1}(\sigma/\sigma_{\mathrm{tr}}) - z/\lambda_s]\}^{-1}\theta(\sigma - \sigma_{\mathrm{tr}})$, where $s^* = (2b\,\delta\rho/C)^{1/2}$. The magnetic response of the surface can be characterized by the surface density of Bohr magnetons, $\mathfrak{M} = \int_{-\infty}^{0} 2s(z)dz$ [see Fig. 2(d)]: $\mathfrak{M} = \mathfrak{M}^* \log\{\sigma/\sigma_{\mathrm{tr}} + [(\sigma/\sigma_{\mathrm{tr}})^2 - 1]^{1/2}\}\theta(\sigma - \sigma_{\mathrm{tr}})$, where $\mathfrak{M}^* = (2A/C)^{1/2}$. The characteristic magnetization, $\mathfrak{M}^*$, is independent of δT so that the effective magnetic susceptibility to the charging, $\mathfrak{M}^*/\sigma_{\mathrm{tr}} \propto \delta T^{-1/2}$, grows infinitely as one approaches the transition point [see Fig. 2(d) inset].

In reality, the surface charge is limited by the breakdown of the insulating interface material. For SiO_2, the breakdown electric field $E_{SiO_2} \approx 10^7$ V/cm, which corresponds to the following charging $\sigma_{SiO_2} = \epsilon E_{SiO_2}/(4\pi e) \approx 2.5 \times 10^{13}\ \text{cm}^{-2}$, where $\epsilon = 4.5$ is the SiO_2 dielectric constant. According to our estimations, for the $Ni_{1-x}Cu_x/SiO_2$ interface, which is $\delta T = 5$ K away from the transition, the threshold charging $\sigma_{tr} \approx 0.15 \times \sigma_{SiO_2}$, and on the edge of the semiconductor breakdown ($\sigma \lesssim \sigma_{SiO_2}$) the surface magnetization is $\mathfrak{M} \approx 1.3 \times 10^{14}\ \mu_B\ \text{cm}^{-2}$.

The magnetic properties of the surface are in fact different from the bulk on their own, without charging. This difference is modeled in the surface phase transition theory as a delta-functional jump of the local Curie temperature at the surface of the semi-infinite system (see, e.g., Ref. 13 and references therein). Within the proposed approach the jump can be taken into account as an intrinsic shift of the charging density $\sigma \rightarrow \sigma_{int} + \sigma$ (the cases $\sigma_{int} \gtrless 0$ are known, respectively, as ordinary and extraordinary transitions). A reliable estimate for the material- and interface-dependent σ_{int} can only be obtained from *ab-initio* studies or experimental data.

Another issue is the quantum fluctuations, due to which the critical exponent of the spin correlation length must acquire the renormalization group correction: $\lambda_s \rightarrow \lambda_s^* \approx \lambda_\rho (T_C/\delta T)^{1/2+\delta}$ ($\delta \approx 0.14$ for, e.g., the $d = 4 - \epsilon$ approximation[14]). Accordingly, the exponential tail of the magnetization profile will be elongated and the magnetic response should acquire an enhancement factor $\propto (T_C/\delta T)^\delta$. On the other hand, the intrinsic substitutional irregularity in a solid solution must shorten λ_s due to the Anderson localization mechanism. Near the transition, the quantum fluctuations' effect is dominant, and in reality the magnetic response of the surface is stronger than the one obtained here on the mean-field level.

The authors are grateful to Lu J. Sham, Alan H. MacDonald, and Daniel Neuhauser for useful comments and discussions. The work was supported in part by Western Institute of Nanoelectronics at UCLA.

---

[*] iovchinnikov@ucla.edu
[†] wang@ee.ucla.edu

[1] S. A. Wolf, D. D. Awschalom, R. A. Buhrman, J. M. Daughton, S. von Molnar, M. L. Roukes, A. Y. Chtchelkanova, and D. M. Treger, Science **294**, 1488 (2001).

[2] Y. D. Park, A. T. Hanbicki, S. C. Erwin, C. S. Hellberg, J. M. Sullivan, J. E. Mattson, T. F. Ambrose, A. Wilson, G. Spanos, and B. T. Jonker, Science **295**, 651 (2002); I. Žutić, J. Fabian, and S. Das Sarma, Rev. Mod. Phys. **76**, 323 (2004); A. H. MacDonald, P. Schiffer, and N. Samarth, Nat. Mater. **4**, 195 (2005); T. Jungwirth, J. Sinova, J. Masek, J. Kucera, and A. H. MacDonald, Rev. Mod. Phys. **78**, 809 (2006).

[3] H. Ohno, D. Chiba, F. Matsukura, T. Omiya, E. Abe, T. Dietl, Y. Ohno, and K. Ohtani, Nature (London) **408**, 944 (2000).

[4] E. C. Stoner, Proc. R. Soc. London, Ser. A **165**, 372 (1938); E. P. Wohlfarth, *ibid.* **195**, 434 (1949).

[5] S. A. Ahern, M. J. Martin, and W. Sucksmith, Proc. R. Soc. London, Ser. A **248**, 145 (1958).

[6] L. Michalak, C. M. Canali, and V. G. Benza, Phys. Rev. Lett. **97**, 096804 (2006); S. Kleff, J. von Delft, M. M. Deshmukh, and D. C. Ralph, Phys. Rev. B **64**, 220401(R) (2001); C. M. Canali and A. H. MacDonald, Phys. Rev. Lett. **85**, 5623 (2000).

[7] To avoid confusion, even though $\epsilon_F^\uparrow > \epsilon_F^\downarrow$ for ferromagnetic states, the total *kinetic-exchange* Fermi energies are, of course, the same and equal the chemical potential.

[8] In fact, the paramagnetic solution always exists. In the ferromagnetic region, however, the paramagnetic solution is unstable with respect to fluctuations in s_0 (the Stoner criterion): $\partial^2 \mathcal{E}_{\mathcal{KX}}/\partial s_0^2|_{s_0=0} < 0$.

[9] D. A. Papaconstantopoulos, *Handbook of the Band Structure of Elemental Solids* (Plenum, New York, 1986). In the estimations, the position of the 3d band edge, ϵ_{3d}, is taken to be at the energy of the $X5$ k-point, ϵ_{X5}: $\mu_P(\rho_{Ni,Cu}) - \epsilon_{3d} \approx -0.21$ eV and 1.57 eV, respectively; the exchange splitting in Ni is: $\epsilon_{X5}^\downarrow - \epsilon_{X5}^\uparrow \approx 0.82$ eV.

[10] R. G. Parr and W. Yang, *Density-Functional Theory of Atoms and Molecules* (Oxford University Press, New York, 1989).

[11] I. V. Ovchinnikov, L. A. Bartell, and D. Neuhauser, J. Chem. Phys. **126**, 134101 (2007).

[12] S. Prakash and S. K. Joshi, Phys. Rev. B **2**, 915 (1970).

[13] H. W. Diehl, in *Phase Transitions and Critical Phenomena*, edited by C. Domb and J. L. Lebowitz (Academic, London, 1986), Vol. 10.

[14] S. K. Ma, Rev. Mod. Phys. **45**, 589 (1973).